Appendix I: Bloch Sphere Representation

The Bloch sphere provides an extremely useful geometrical representation of the state of a spin-1/2 system. We consider a ground state $|\uparrow\rangle$ and excited state $|\downarrow\rangle$. Any (normalized) superposition state can be expressed as follows:

$$|\psi\rangle = \cos\frac{\theta}{2}|\uparrow\rangle + \sin\frac{\theta}{2}\,e^{i\phi}|\downarrow\rangle, \tag{1}$$

where θ and ϕ are real. The parameter θ expresses the relative amplitude of the basis states, while ϕ expresses their relative phase. In the Bloch sphere representation, the state $|\psi\rangle$ is depicted as a vector pointing from the origin to a point on the surface of the unit sphere; the direction of the state vector is specified by polar angle θ and azimuthal angle ϕ. For example, the ground state $|\uparrow\rangle$ resides at the north pole of the Bloch sphere, the excited state $|\downarrow\rangle$ resides at the south pole, while an equal superposition of $|\uparrow\rangle$ and $|\downarrow\rangle$ exists somewhere on the equator (Fig. 1).

In general, the state of the spin will be a statistical mixture of pure states of the form (1) (a so-called "mixed state"). In this case, the state is described by a 2x2 density matrix, involving three real parameters. The state of the system can be depicted as a vector with polar and azimuthal angles θ and ϕ and length $r < 1$. Thus, a mixed state resides in the interior of the Bloch sphere. For example, an incoherent mixture of spin-up and spin-down with equal weights (corresponding to an infinite spin temperature) is described by the density operator

$$\rho = \frac{1}{2}|\uparrow\rangle\langle\uparrow| + \frac{1}{2}|\downarrow\rangle\langle\downarrow|; \tag{2}$$

this state is depicted as a point at the origin of the Bloch sphere.

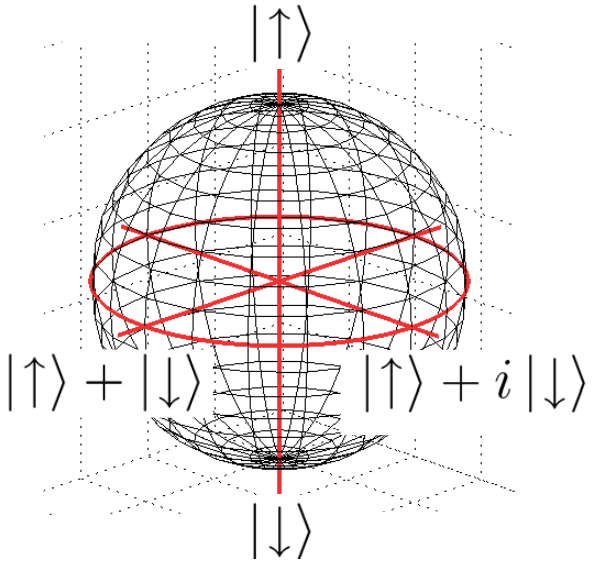

Figure 1: Bloch sphere representation of a spin-1/2 system.

Spin Rotations

When the spin-1/2 system is immersed in a static field $\mathbf{B} = B_0\,\hat{z}$, the moments become polarized along the Zeeman field direction. To induce spin flips, we apply a weak, oscillating magnetic field in the xy plane, at a frequency $\omega_0 \equiv B_0/\gamma$ that is matched to the Zeeman splitting, where γ is the nuclear gyromagnetic ratio. Most often this excitation field is linearly polarized; for example, it is typically produced by a small solenoid coupled tightly to the spin sample and oriented in a direction orthogonal to the Zeeman field. The linearly polarized excitation can be decomposed into two counter-rotating components that circulate at angular frequency $\pm\omega_0$. The effect of the excitation field is best understood by transforming to a reference frame that rotates with the excitation component that is matched to the sense of spin precession. In this frame, one component of the excitation field appears stationary, while the counter-rotating component circulates at twice the Larmor frequency and can be neglected. By Larmor's theorem, transformation to the rotating frame is equivalent to the application of a magnetic field $-\gamma\,\omega_0\,\hat{z}$ that cancels the Zeeman field. In the absence of a Zeeman field, the spins experience a torque due to the stationary component of the excitation field that can tip the moments away from the $\hat{z}$ direction.

In the Bloch sphere representation, the excitation field corresponds to a control vector aligned in the equatorial plane that induces rotations of the sample magnetization. The orientation of the control vector is related to the phase of the radiofrequency excitation field (for example, by introducing 90° phase shifts between resonant pulses, it is possible to perform rotations about both the $x-$ and $y-$axes of the Bloch sphere), while the length of the control vector is determined by the magnitude B_1 of the excitation field in the rotating frame. Under the influence of the excitation field, the sample magnetization rotates at a frequency

$$\omega_1 = \gamma B_1. \tag{3}$$

The tip angle θ_{pulse} of the excitation pulse is determined by the integral

$$\theta_{pulse} = \gamma \int B_1(t)\,dt. \tag{4}$$

Appendix II: Spin Relaxation

In NMR we distinguish two distinct types of spin relaxation: (1) longitudinal relaxation, corresponding to decay of the excited state and relaxation of the state vector toward thermal equilibrium, and (2) transverse relaxation, corresponding to decay of the transverse (xy) components of the state vector. Relaxation of the spin magnetization $\boldsymbol{M}$ is described by the phenomenological Bloch equations:

$$\begin{aligned} \frac{dM_z}{dt} &= \frac{M_{z,0} - M_z}{T_1} \\ \frac{dM_{x,y}}{dt} &= \frac{-M_{x,y}}{T_2}, \end{aligned} \tag{5}$$

where $M_{z,0}\,\hat{z}$ is the equilibrium spin magnetization and where T_1 and T_2 are the longitudinal (or spin-lattice) and transverse (or spin-spin) relaxation times, respectively.

Physically, both longitudinal and transverse relaxation are due to fluctuating magnetic fields of microscopic origin that induce spurious rotations of the state vector on the Bloch sphere. Longitudinal relaxation involves a transfer of population from $|\downarrow\rangle$ to $|\uparrow\rangle$, and requires the exchange of quanta with a thermal reservoir (the "lattice"). Thus, T_1 processes involve fluctuations at the Larmor frequency, corresponding to rotations about a control vector oriented in the transverse ($xy-$) plane of the Bloch sphere. These high-frequency, resonant fluctuations also contribute to transverse relaxation; in this case, however, only one quadrature of the fluctuating field can induce a spurious rotation of the transverse magnetization, since a control vector that is aligned with the magnetization induces no rotation. At the same time, energy-conserving, low-frequency fluctuations of the $z-$component of the magnetic field also produce transverse relaxation, with a characteristic *pure dephasing time* T_2'. The transverse relaxation time T_2 is related to T_1 and T_2' as follows:

$$\frac{1}{T_2} = \frac{1}{2T_1} + \frac{1}{T_2'}. \tag{6}$$

Relaxation in Liquids

For many nuclear spin samples of interest, the fluctuating fields that induce relaxation are due to nearby nuclear spins that are oriented randomly with respect to the Zeeman field direction (recall that for typical temperatures and Zeeman field strengths, the nuclear spin polarization is quite small, of order $10^{-6} - 10^{-5}$). To estimate the magnitude of this effect, we calculate the dipolar field B_{loc} of a proton at a distance $r = 1$ Å. We find

$$B_{loc} \approx \frac{\mu_0 \mu_p}{4\pi r^3} = 1\,\mathrm{mT}. \tag{7}$$

These local fields cause spins to acquire a spurious phase at characteristic rate

$$\omega_{loc}/2\pi = B_{loc}/2\pi\gamma \approx 40\,\mathrm{kHz}. \tag{8}$$

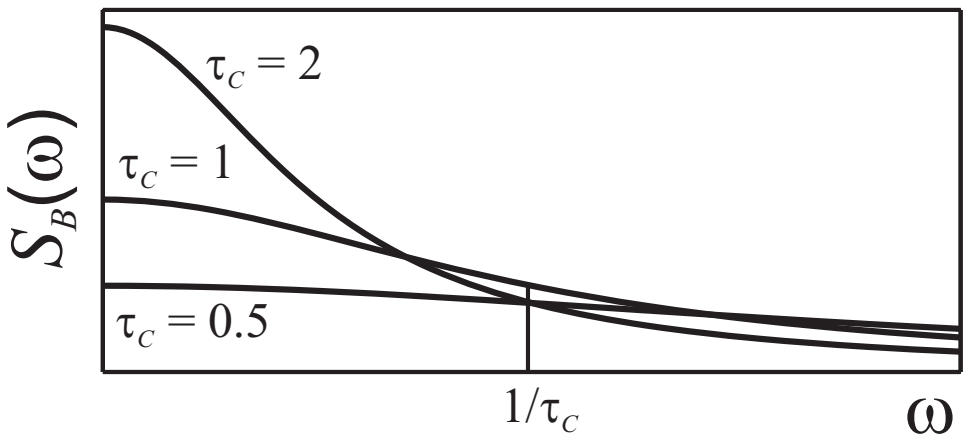

Figure 2: Spectral density of local field fluctuations for different molecular correlation times τ_c (arbitrary units).

Since each spin acquires phase at a random rate (due to the random orientations and magnitudes of local fields), phase coherence is lost in a characteristic time $1/\omega_{loc}$ of order 1-10 microseconds.

The above picture of fixed, randomly oriented nuclei is valid in the case of a nuclear spin sample in the solid state, where the molecules are rigidly bound in the lattice. For nuclei in a liquid sample, the rapid reorientation of the molecules causes randomization of the local magnetic field experienced by each nucleus on a timescale τ_c, the microscopic correlation time characteristic of molecular rotations. As a result, each spin accumulates spurious phase at a much slower rate, leading to a dramatic increase in spin relaxation times and a corresponding narrowing of the NMR lines, an effect known as *motional narrowing*. The following simplified picture (after C. Kittel, *Introduction to Solid-State Physics*) provides physical intuition. We consider spin dephasing in the liquid state in terms of a one-dimensional random walk of the phase θ of the nuclear spin. We break the time axis into discrete steps of duration τ_c; during each time step, the spin acquires phase $\pm\omega_{loc}\tau_c$, where the sign is random. After N time steps, the spin has acquired a spurious phase

$$\theta(N) \approx \sqrt{N}\omega_{loc}\tau_c. \tag{9}$$

Phase coherence is lost when the spurious phase is of order 1, i.e., after $N \approx (\omega_{loc}\tau_c)^{-2}$ time steps. The spin dephasing time is therefore

$$T_2' \approx \frac{1}{\omega_{loc}^2\tau_c}. \tag{10}$$

We see that the spin relaxation time in the liquid is enhanced by a factor $1/\omega_{loc}\tau_c$ over its value in the solid state. For water at room temperature, we have $1/\omega_{loc} \approx 10$ μs and $\tau_c \approx 100$ ps; thus, we expect spin relaxation times of order 1 s, an enhancement of about five orders of magnitude over the relaxation times seen in the solid state.

In a more rigorous treatment, one can show that the longitudinal relaxation rate is proportional to the spectral density $S_B(\omega_0)$ of local magnetic field fluctuations at the Larmor

frequency, while the pure dephasing rate is proportional to the spectral density $S_B(0)$ of field fluctuations at zero frequency:

$$\begin{aligned} 1/T_1 &= 2\pi\gamma^2 S_B(\omega_0) \\ 1/T_2' &= \pi\gamma^2 S_B(0). \end{aligned} \tag{11}$$

In a liquid, the field fluctuations are due to the random tumbling of the molecules, resulting in the rapid translation and rotation of the nuclear dipole moments. The random motion of the molecules causes an exponential decay of the autocorrelation function of the local magnetic field, with characteristic time τ_c:

$$< B(0)B(t) >= B_{loc}^2 e^{-t/\tau_c}. \tag{12}$$

The Fourier transform of the autocorrelation yields the power spectral density of magnetic field fluctuations:

$$S_B(\omega) = B_{loc}^2 \frac{\tau_c}{1+\omega^2\tau_c^2}. \tag{13}$$

As τ_c increases, weight in the fluctuation spectrum is shifted from high frequency to low frequency, but the total noise power is conserved (Fig. 2). Clearly, T_2' decreases monotonically as τ_c increases; this makes sense, since motional narrowing becomes less effective as molecular motion slows. On the other hand, T_1 goes through a local minimum as τ_c increases. Spin-lattice relaxation is most efficient when τ_c is matched to the inverse of the Larmor frequency.

When the Larmor frequency is much less than the inverse correlation time (a situation that is often realized in liquids), we have

$$S_B(0) \approx S_B(\omega_0). \tag{14}$$

Combining Equations 6, 11, and 14 above, we find

$$T_2 \approx T_1. \tag{15}$$

In this laboratory, you will use inversion-recovery sequences to measure T_1, and spin-echo (or CPMG) sequences to measure T_2. The liquid samples will span a range of viscosities, corresponding to a range of rotational correlation times. For a liquid with molecules approximated as spheres with radius a, the correlation time τ_c is related to viscosity η as follows:

$$\tau_c = \frac{4\pi\eta a^3}{3k_B T}. \tag{16}$$

Because $1/T_1 \propto \tau_c$ and $\tau_c \propto \eta$, we have $T_1 \propto 1/\eta$. Figure 3 demonstrates this relationship for water-glycerine mixtures spanning three orders of magnitude in viscosity.

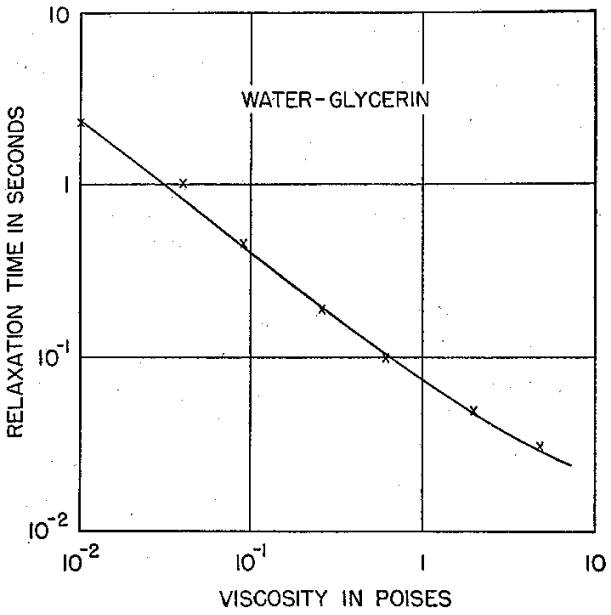

Figure 3: NMR relaxation times in water-glycerine mixtures at 29 MHz (from Bloembergen).

Procedure

1. Calculate the thermal polarization of proton spins at room temperature in a magnetic field of 0.35 T.

2. Using the mineral oil sample, adjust the excitation frequency until you find the proton resonance (note that the oscillations at the mixer output are at the difference between the excitation frequency and the Larmor frequency). Estimate the inhomogeneous linewidth of the proton resonance.

3. Employ the CPMG sequence to measure T_2 of the following samples: mineral oil, and 100%, 80%, and 50% glycerine solutions in water. Make careful note of the pulse sequence parameters, and check that the repetition rate is low enough that the spins are properly initialized before the 90° pulse.

4. Use inversion-recovery sequences to measure the T_1 times of the above samples.

5. Explain the dependence of spin relaxation time on glycerine concentration for the glycerine-water solutions. Refer to the table below (from Bloembergen).

Viscosity of Aqueous Glycerine Solutions in Centipoises/mPa s

Glycerine per cent weight	Temperatur e (°C)										
	0	10	20	30	40	50	60	70	80	90	100
0 [1]	1.792	1.308	1.005	0.8007	0.6560	0.5494	0.4688	0.4061	0.3565	0.3165	0.2838
10	2.44	1.74	1.31	1.03	0.826	0.680	0.575	0.500	–	–	–
20	3.44	2.41	1.76	1.35	1.07	0.879	0.731	0.635	–	–	–
30	5.14	3.49	2.50	1.87	1.46	1.16	0.956	0.816	0.690	–	–
40	8.25	5.37	3.72	2.72	2.07	1.62	1.30	1.09	0.918	0.763	0.668
50	14.6	9.01	6.00	4.21	3.10	2.37	1.86	1.53	1.25	1.05	0.910
60	29.9	17.4	10.8	7.19	5.08	3.76	2.85	2.29	1.84	1.52	1.28
65	45.7	25.3	15.2	9.85	6.80	4.89	3.66	2.91	2.28	1.86	1.55
67	55.5	29.9	17.7	11.3	7.73	5.50	4.09	3.23	2.50	2.03	1.68
70	76	38.8	22.5	14.1	9.40	6.61	4.86	3.78	2.90	2.34	1.93
75	132	65.2	35.5	21.2	13.6	9.25	6.61	5.01	3.80	3.00	2.43
80	255	116	60.1	33.9	20.8	13.6	9.42	6.94	5.13	4.03	3.18
85	540	223	109	58	33.5	21.2	14.2	10.0	7.28	5.52	4.24
90	1310	498	219	109	60.0	35.5	22.5	15.5	11.0	7.93	6.00
91	1590	592	259	127	68.1	39.8	25.1	17.1	11.9	8.62	6.40
92	1950	729	310	147	78.3	44.8	28.0	19.0	13.1	9.46	6.82
93	2400	860	367	172	89	51.5	31.6	21.2	14.4	10.3	7.54
94	2930	1040	437	202	105	58.4	35.4	23.6	15.8	11.2	8.19
95	3690	1270	523	237	121	67.0	39.9	26.4	17.5	12.4	9.08
96	4600	1580	624	281	142	77.8	45.4	29.7	19.6	13.6	10.1
97	5770	1950	765	340	166	88.9	51.9	33.6	21.9	15.1	10.9
98	7370	2460	939	409	196	104	59.8	38.5	24.8	17.0	12.2
99	9420	3090	1150	500	235	122	69.1	43.6	27.8	19.0	13.3
100	12070	3900	1410	612	284	142	81.3	50.6	31.9	21.3	14.8

[1] Viscosity of water taken from "Properties of Ordinary Water-Substance." N.E. Dorsey, p. 184. New York (1940)

Figure 4: